Original Article

In vitro elastic cartilage reconstruction using human auricular perichondrial chondroprogenitor cell–derived micro 3D spheroids

Journal of Tissue Engineering
Volume 13: 1–13

DOI: 10.1177/20417314221143484
journals.sagepub.com/home/tej
SAGE

Takayoshi Oba[1,2], Satoshi Okamoto[1], Yasuharu Ueno[3], Megumi Matsuo[1], Tomomi Tadokoro[1], Shinji Kobayashi[4], Kazunori Yasumura[4], Shintaro Kagimoto[5], Yutaka Inaba[2] and Hideki Taniguchi[1,3]

Abstract

Morphologically stable scaffold-free elastic cartilage tissue is crucial for treating external ear abnormalities. However, establishing adequate mechanical strength is challenging, owing to the difficulty of achieving chondrogenic differentiation in vitro; thus, cartilage reconstruction is a complex task. Auricular perichondrial chondroprogenitor cells exhibit high proliferation potential and can be obtained with minimal invasion. Therefore, these cells are an ideal resource for elastic cartilage reconstruction. In this study, we aimed to develop a novel in vitro scaffold-free method for elastic cartilage reconstruction, using human auricular perichondrial chondroprogenitor cells. Inducing chondrogenesis by using microscopic spheroids similar to auricular hillocks significantly increased the chondrogenic potential. The size and elasticity of the tissue were maintained after craniofacial transplantation in immunodeficient mice, suggesting that the reconstructed tissue was morphologically stable. Our novel tissue reconstruction method may facilitate the development of future treatments for external ear abnormalities.

Keywords

Elastic cartilage, rotating culture, microtia, auricular perichondrial chondroprogenitor cells, micro three-dimensional culture

Date received: 11 October 2022; accepted: 19 November 2022

Introduction

Microtia, characterized by a small, abnormally shaped auricle, is one of the most common external ear abnormalities, with an incidence of 1–10 per 10,000 births.[1–3] Auto-transplantation of costal cartilage segments is one of the most popular treatments. However, this strategy has disadvantages, such as the lack of elasticity of costal cartilage, difficulty in harvesting costal cartilage, and post-operative pain at the donor site.[4,5] To this end, elastic cartilage engineering methods involving scaffolds, such as polyglycolic acid and polylactic acid, have been developed.[6–10] However, post-operative problems such as rejection and deformation of the materials can occur.[10–13] Scaffold-free elastic cartilage has been constructed using auricular chondrocytes but has not been evaluated in vivo.[14,15] Therefore, a system for establishing morphologically stable scaffold-free elastic cartilage amenable to in vivo evaluation is necessary.

[1]Department of Regenerative Medicine, Graduate School of Medicine, Yokohama City University, Kanazawa-ku, Yokohama, Japan
[2]Department of Orthopaedic Surgery, Yokohama City University, Kanazawa-ku, Yokohama City, Kanagawa, Japan
[3]Division of Regenerative Medicine, Center for Stem Cell Biology and Regenerative Medicine, The Institute of Medical Science, the University of Tokyo, Minato-ku, Tokyo, Japan
[4]Department of Plastic and Reconstructive Surgery, Kanagawa Children's Medical Center, Minami-ku, Yokohama, Kanagawa, Japan
[5]Department of Plastic and Reconstructive Surgery, Yokohama City University, Kanazawa-ku, Yokohama, Kanagawa, Japan

Corresponding authors:
Takayoshi Oba, Department of Regenerative Medicine, Graduate School of Medicine, Yokohama City University, 3-9 Fukuura, Kanazawa-ku, Yokohama 236-0004, Japan.
Email: t186017g@yokohama-cu.ac.jp

Hideki Taniguchi, Division of Regenerative Medicine, Center for Stem Cell Biology and Regenerative Medicine, The Institute of Medical Science, the University of Tokyo, 4-6-1 Shirokanedai, Minato-ku, Tokyo 108-8639, Japan.
Email: rtanigu@ims.u-tokyo.ac.jp

In our previous study, we succeeded in developing a method for creating scaffold-free elastic cartilage in vivo.[16] However, the tissue shrank to approximately half its initial size during transplantation.[16] Mesenchymal aggregation, which occurs during cartilage differentiation, may explain this shrinkage.[17,18] Therefore, a method in which cartilage differentiation is mostly completed in vitro is required. The cell type used for reconstruction is another important matter in elastic cartilage engineering. While most studies have used auricular chondrocytes, CD44+CD90+ chondroprogenitor cells found in the auricular perichondrium have been reported to be an ideal resource, as they exhibit a high proliferation capacity and can be obtained with minimal invasion.[19,20]

In this study, we aimed to develop an in vitro method for reconstructing morphologically stable elastic cartilage, using human auricular perichondrial chondroprogenitor cells. To improve the in vitro culturing conditions, we focused on mimicking the morphological aspects of chondrogenic induction during early auricular development. The development of the human auricular cartilage begins with the emergence of six round 200–300 μm structures with a mesenchymal character, termed "auricular hillocks," at 6 weeks gestation (Figure 1(a)).[21–23] The three anterior hillocks (hillocks 1–3) are derived from the first pharyngeal arch, and the three posterior hillocks (hillocks 4–6) are derived from the second pharyngeal arch; both arches originate from the migrating neural crest cells. The hillocks then fuse together, creating the complex auricle structure.[21–23] Previous studies of elastic cartilage tissue engineering have achieved chondrogenic induction by creating macro-level structures.[6–15] We hypothesized that chondrogenic induction could be improved by mimicking the auricular hillock morphologically, using Φ200–300 μm spheroid culture plates (micro 3D culture).

We compared the chondrogenic induction efficacy of micro 3D culture with that of petri dish culture (2D culture) and Φ1000–2000 μm spheroid culture (macro 3D culture). Micro 3D–cultured spheroids were fused together to form a tissue large enough for manipulation and then cultured in a rotating wall vessel. Histological and morphological evaluation of the reconstructed elastic cartilage was performed, and the reconstructed cartilage was compared with human native auricular cartilage. Finally, the morphological stability of the elastic cartilage tissue after craniofacial transplantation was examined in immunodeficient mice.

Material and methods

Observation of auricular hillocks in mouse embryos

Pregnant wild-type mice were purchased from Japan SLC. E10.5, E11, E11.5, and E12 mouse embryos were collected, and the amniotic membrane was peeled off microscopically. After microscopic pictures of the auricular hillocks were taken, the embryos were placed in 4% paraformaldehyde for whole-mount immunohistochemistry.

Isolation of auricular chondroprogenitor cells

Elastic cartilage samples were obtained from microtia patients following the approved guidelines set by the ethical committee at Yokohama City University Graduate School of Medicine Hospital (approval no. B130905006). Auricular chondroprogenitor cells in the perichondrium were isolated using previously reported methods.[16,20] In brief, auricular tissue samples from microtia patients were microscopically separated into the chondral layer, the interlayer, and the perichondral layer. The perichondral samples were minced into a paste and centrifuged at 37°C and 600 rpm for 2 h to isolate the perichondrial cells. The suspension was then filtered through a 40 μm cell strainer and centrifuged at 1500 rpm for 5 min. The collected cells were resuspended in DMEM containing 10% fetal bovine serum (FBS) and cultured in a 35 mm dish until confluent. This was defined as passage 0.

Flow cytometry

The expression of the auricular perichondrial chondroprogenitor cell markers CD90, CD44, CD73, and CD105 on the cell membrane was analyzed in perichondrial cells (passage 0) using flow cytometry. The perichondrial cells were washed with Dulbecco's phosphate-buffered saline (DPBS) and dissociated into single cells with 0.25% trypsin. The cells were collected by centrifugation, resuspended in DPBS with 1% bovine serum albumin (FACS buffer), and incubated with antibodies for 30 min at 4°C. After the cells were washed three times with FACS buffer, the fluorescence of the cell membrane was detected using the Cell Sorter MA900 (Sony). See Supplemental Figure 1(a) for the gating process, and Supplemental Table 1 for antibody information.

Cell expansion culture

The confluent perichondrial cells were dissociated into single cells with 0.25% trypsin. Next, 50,000 cells were seeded in a 100 mm dish containing Dulbecco's Modified Eagle's Medium (DMEM)/F12 Ham (1:1) (Sigma-Aldrich), stabilized antibiotic–antimycotic solution (100×) (Sigma-Aldrich), 0.2 mM ascorbic acid 2-phosphate (AA2P) (Sigma-Aldrich), 10^{-7} M dexamethasone (Sigma-Aldrich), 1× ITS-X (Gibco), 5 ng/mL insulin-like growth factor (IGF) (Sigma-Aldrich), 10 ng/mL basic fibroblast growth factor (FGF) (Wako), 10 ng/mL platelet-derived growth factor BB (PDGF-BB) (Peprotech), and 2% FBS. The medium was changed every other day until the cells became confluent, which occurred between 7 and 10 days of culture (passage 1 cells).

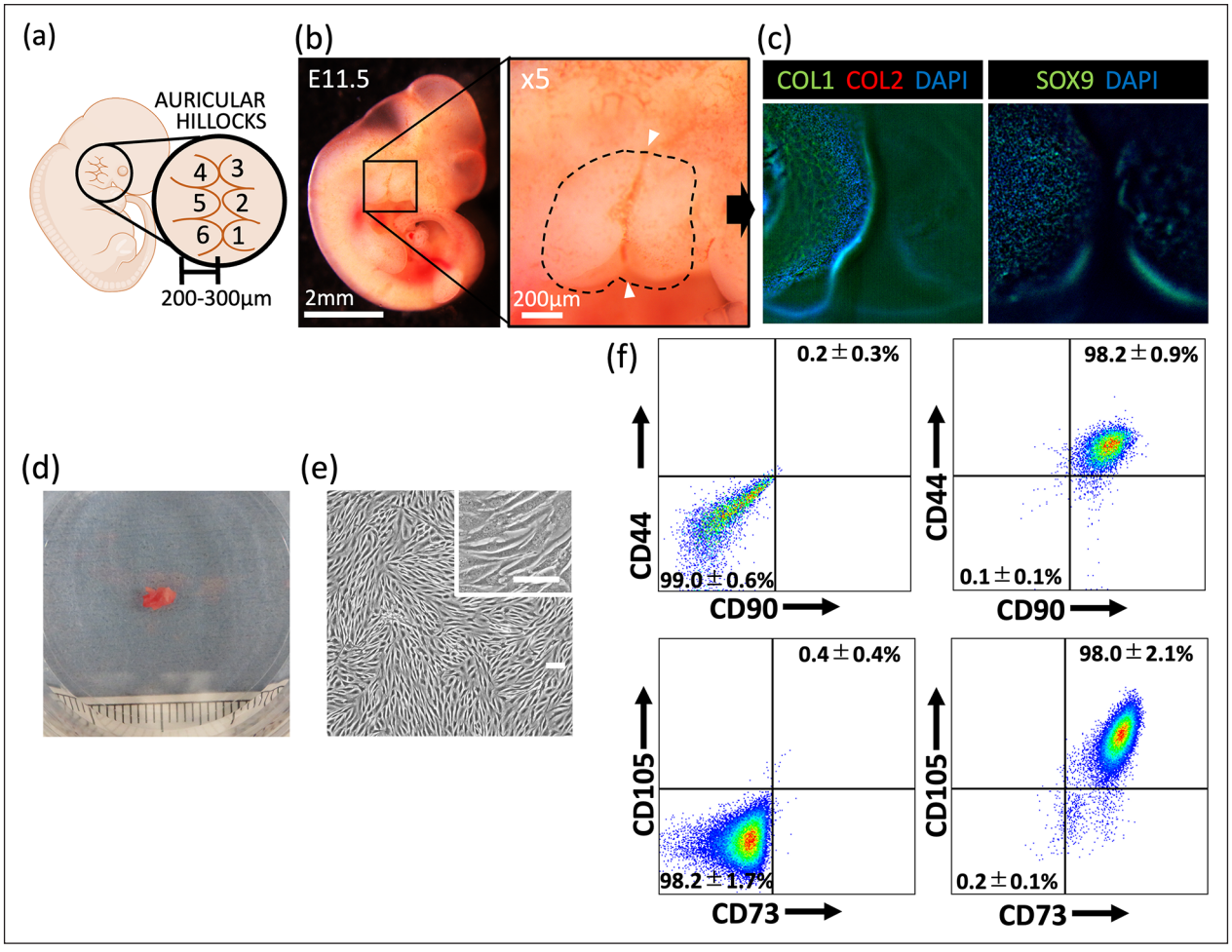

Figure 1. Analysis of fetal auricular hillocks and human perichondrial chondroprogenitor cells. (a) Schematic representation of a human embryo at 6 weeks gestation, showing the emerging auricular hillocks. (b) Image of the auricular hillocks of an E11.5 mouse embryo, with a magnified view shown on the right. Dashed line indicates the outline of the hillocks. White arrowheads indicate the first pharyngeal groove. (c) Immunohistochemistry of E11.5 mouse embryonic auricular hillocks. Left panel: type I collagen (COL1) (green), type II collagen (COL2) (red), and diamidino-phenylindole (DAPI) (blue) staining; right panel: SOX9 and DAPI staining. (d) Image of an excised auricular perichondrium (scale: 1 mm). (e) Image of expanded auricular perichondrial chondroprogenitor cells (scale bars: 100 μm). (f) Representative flow cytometry analysis of perichondrial cells to determine CD44, CD90, CD73, and CD105 expression in four patient samples. Left panels: unstained cells (negative control). Data are shown as the mean ± SD.

Chondrogenic induction culture

The following three culture methods are described: 2D culture, micro 3D culture, and macro 3D culture. The expanded auricular perichondrial chondroprogenitor cells (passage 1) were dissociated into single cells with 0.25% trypsin. For 2D culture, 30,000 cells were seeded into a well of a 24-well plate containing 300 μL of chondrogenic induction medium comprising DMEM/F12 Ham (1:1) (Sigma-Aldrich), stabilized antibiotic–antimycotic solution (100×) (Sigma-Aldrich), 0.2 mM AA2P (Sigma-Aldrich), 10^{-7} M dexamethasone (Sigma-Aldrich), 1× ITS-X (Gibco), 5 ng/mL IGF (Sigma-Aldrich), 10 ng/mL basic FGF (Wako), 10 ng/mL PDGF-BB (Peprotech), 10 ng/mL transforming growth factor β1 (TGFβ1) (Peprotech), and 2% FBS.

For micro 3D culture, 30,000 cells in 300 mL of chondrogenic induction medium were divided into two wells of a 96-well U-bottomed micropatterned plate (Corning). Each well of the U-bottomed micropatterned plate had 79 micro-wells. Thus, 158 micro-wells were used, and each micro-well contained 190 cells. For macro 3D culture, 30,000 cells in 300 μL of chondrogenic induction medium were seeded into a well of a 96-well U-bottomed plate (Greiner Bio-One). The medium in each culture system was carefully changed daily. After a culture duration of 1, 3, and 5 days, cells were collected for analysis in each culture system.

Rotating wall vessel culture

Approximately 3000 spheroids from day 3 micro 3D culture were collected from the micropatterned plate by gentle pipetting and transferred to a rotating wall vessel containing 50 mL of chondrogenic induction medium. The spheroids were kept still overnight to allow fusion, followed by rotating culture at 15 rpm. The following week, the medium was replaced with chondrogenic induction medium containing DMEM/F12 Ham (1:1) (Sigma-Aldrich), stabilized antibiotic–antimycotic solution (100×) (Sigma-Aldrich), 0.2 mM AA2P (Sigma-Aldrich), 10^{-7} M dexamethasone (Sigma-Aldrich), 1× ITS-X (Gibco), 5 ng/mL IGF (Sigma-Aldrich), 10 ng/mL basic FGF (Wako), 10 ng/mL PDGF-BB (Peprotech), 10 ng/nL TGFβ1 (Peprotech), 20 ng/mL bone morphogenetic protein 4 (R&D), 1% Glutamax (Gibco), and 1% FBS. The medium was changed weekly for a total of 4 weeks.

Animal experiments

Eight-week-old female NOD/Scid mice were purchased from Oriental Yeast Co. After anesthetization, hair around the forehead was removed, and the skin was sanitized with 70% ethanol. A horizontal incision was made in the posterior forehead, and a subcutaneous space was created by anteriorly inserting a spatula. In the treatment group, the reconstructed elastic cartilage was inserted into the created space with ring tweezers. The incision was closed with 6-0 silk thread sutures. Using a caliper, the thickness of the transplanted cartilage and skin was measured in the treatment group, and pinched skin was measured in the sham group. After a 2-month transplantation period, the mice were sacrificed, and the elastic cartilage was excised for further analysis.

Size measurements

The diameters of the micro 3D–cultured spheroids, macro 3D–cultured spheroids, in vitro elastic cartilage, and ex vivo elastic cartilage were calculated by taking the mean of the maximum and minimum Feret diameters of images obtained using ImageJ software.

Quantitative reverse transcription-polymerase chain reaction (qRT-PCR)

Total RNA was extracted using the PureLink RNA mini kit (Thermo Fisher Scientific). Total RNA was reverse transcribed into cDNA using a Thermal Cycler TP600 (Takara) and High-Capacity cDNA Reverse Transcription Kit with random primers (Thermo Fisher Scientific). cDNA samples were mixed with THUNDERBIRD Probe qPCR Mix (Toyobo), Taqman probe (Universal Probe Library; Roche), and gene-specific primers. As an internal reference, Eukaryotic 18S rRNA Endogenous Control (Thermo Fisher Scientific) was used. Thermal cycling was performed using the Light Cycler 480 system (Roche). The gene expression levels were quantified using the ΔΔCp method. The primers used are shown in Supplemental Table 1.

Enzyme linked immuno-sorbent assay (ELISA)

For measurements of secreted melanoma inhibitory activity (MIA) levels and hyaluronic acid (HA) levels, the DuoSet capture, detection, and standard kits were used (R&D Systems). The blank, standard, and sample (100 μL each) were dispensed into a 96-well plate. Capture reagent (100 μL) was added to each well, which were then kept at room temperature overnight. For washing, 200 μL of 0.1% Tween 20 in PBS (PBS-T) was used. After each well was washed three times, 300 μL of Block Ace (DC Pharma) was added, and the wells were kept at room temperature for 1 h. Each well was washed again three times. Next, 100 μL each of the blank, standard, and sample was added to the 96-well plate, which was kept at room temperature for 2 h. Each well was washed three times. Next, 100 μL of Detection regent (R&D Systems) was added, and the wells were kept at room temperature for 2 h. Each well was washed three times. Then, 100 μL of Diluted Streptavidin-HRP (R&D Systems) was added, and the wells were kept at room temperature for 20 min. The wells were washed three times, and 100 μL of Substrate solution (R&D Systems) was added. The wells were washed three times, and 50 μL of Stop solution (R&D Systems) was added. MIA and HA levels (450 nm) and reference levels were measured by determining the absorbance with a plate reader (540 or 570 nm). Detailed antibody information is shown in Supplemental Table 1.

Histology and immunohistochemistry

For whole-mount immunostaining of the auricular hillocks of fetal mice, samples were fixed in 4% paraformaldehyde for 2 h. For washing, PBS-T was used. After the samples were washed twice, Protein Block Serum-Free (Dako) was added, and the samples were kept at room temperature for 2 h. The samples were then washed once and incubated with primary antibodies (1:100) for 4 days at 4°C. After they were washed three times, the samples were incubated with secondary antibodies (1:500) overnight at 4°C. After the samples were washed three times, the nuclei were counterstained with diamidino-phenylindole (DAPI) (1:500). Next, the samples were cleared using benzyl alcohol + benzyl benzoate (BABB) (1:1) for microscopic observation. Samples were placed in 50% methanol, 100% methanol, 100% methanol + BABB (1:1), and BABB for 15 min each, respectively.

For immunostaining of 2D-cultured cells, micro 3D–cultured spheroids, and macro 3D–cultured spheroids, the samples were washed with PBS twice and fixed in 4%

paraformaldehyde. After washing with PBS three times, 0.1% Triton/PBS was added, and the samples were incubated at room temperature for 15 min (2D-cultured cells), 30 min (micro 3D–cultured spheroids), or 1 h (macro 3D–cultured spheroids). The samples were washed with PBS three times and placed in PBS with 1% BSA for 10 min. After washing once with PBS, the samples were incubated with primary antibodies (1:200) overnight at 4°C. After washing three times with PBS, the samples were incubated with secondary antibodies (1:1000) for 30 min at room temperature. After washing with PBS three times, the nuclei were counterstained with DAPI.

The in vitro and ex vivo elastic cartilage samples were fixed in 10% formalin and embedded in paraffin. The samples were sliced into 5 μm sections using a microtome. After deparaffinization, the samples were stained with HE, Alcian blue (AB), and Elastica Van Gieson (EVG). For immunohistochemistry, the samples were incubated with primary antibodies (1:200) overnight at 4°C and with secondary antibodies (1:1000) for 30 min at room temperature. Then, the nuclei were counterstained with DAPI. Detailed antibody information is shown in Supplemental Table 1.

Elasticity test

A mechanical stress testing instrument, EZ-Test EZ-SX (Shimadzu), was used to measure the elastic modulus. Samples were set on a pedestal, and a 1 mm diameter jig (Shimazu) was used for compression and detection. The elastic modulus (MPa) at 0.2–0.6 mm was obtained via 3 mm/min indentation and evaluated using Trapezium ver1.4.5 (Shimazu). The measurement was performed three times for each sample, and data were presented as the mean.

Data analysis and statistical methods

The experiment data are presented as the median and interquartile range (IQR), unless otherwise stated. One-way ANOVA followed by Tukey's multiple comparison test was used for comparisons among multiple groups. The Mann–Whitney *U* test was used for comparisons between two groups. Statistical analysis was performed using GraphPad Prism 6.0 (La Jolla, CA, USA). Differences with *p*-values <0.05 were considered statistically significant.

Results

Auricular hillocks in mice embryos

To analyze morphogenesis in early auricular elastic cartilage, we observed the auricular hillocks, which differentiate into auricular cartilage, in E11.5 mouse embryos.[21–23] Morphological characteristics, such as a 200–300 μm diameter, round shape, and adjacent positioning, were moderately consistent with those of human auricular hillocks (Figure 1(b)).[22] Immunohistochemistry analysis indicated that the auricular hillocks were positive for type I collagen (a broad mesenchymal marker) and SOX9 (a craniofacial chondrogenic and mesenchymal condensation marker)[24,25] and negative for type II collagen (a chondrogenic marker). These results were consistent with previous reports that the auricular hillocks are the origin of auricular cartilage and that they exhibit a mesenchymal character at this stage (Figure 1(c), Supplemental Video 1).[23] We hypothesized that elastic cartilage chondrogenesis would be improved by mimicking these morphological features.

Human auricular perichondrial chondroprogenitor cell expansion in 2D culture

After isolation, the auricular perichondrial cells were cultured for 5–7 days until colonies were observed (Figure 1(d) and (e)). The expression of the auricular perichondrial chondroprogenitor markers CD90 and CD44 was detected by flow cytometry.[16,20] CD90+CD44+ auricular perichondrial chondroprogenitor cells comprised 98.2% ± 0.9% of the auricular perichondrial cells. Furthermore, 98.0% ± 2.1% of the auricular perichondrial cells were CD73+CD105+ (Figure 1(f), Supplemental Figure 1(a)). As highlighted by these results, the use of the auricular perichondrium is advantageous because of the high content of stem cells.

Effects of micro 3D culture on elastic cartilage chondrogenesis induction

To mimic the morphology of auricular hillocks, we used a U-bottomed micro-welled plate. Each micro well was 500 μm in diameter and 400 μm in depth, facilitating spheroid creation (Figure 2(a)). We termed this culture method "micro 3D culture." 2D culture (using petri dishes) and macro 3D culture (using a 96-well U-bottomed plate with wells that were 6990 μm in diameter and 10,300 μm in depth) systems were also established. The expression levels of chondrogenic markers and cartilage-related protein secretion were measured to evaluate the effectiveness of each culture system in terms of elastic cartilage chondrogenesis induction (Figure 2(b)). The spheroids observed on days 1, 3, and 5 of micro 3D culture and macro 3D culture were Φ200–300 μm and Φ1000–2000 μm in size, respectively, as expected (Figure 2(c)).

According to the results of qRT-PCR analysis, on days 3 and 5, micro 3D culture induced significantly higher expression of the chondrogenic markers *SOX9* and *COL11A2*, which have crucial roles in craniofacial cartilage development,[24–28] than 2D culture and macro 3D culture (Figure 2(d)). The ELISA results indicated that micro 3D culture induced a significantly higher level of MIA secretion on day 3 than 2D culture and macro 3D culture. On day 3, micro 3D culture also induced a significantly higher level of HA secretion than macro 3D culture, but no

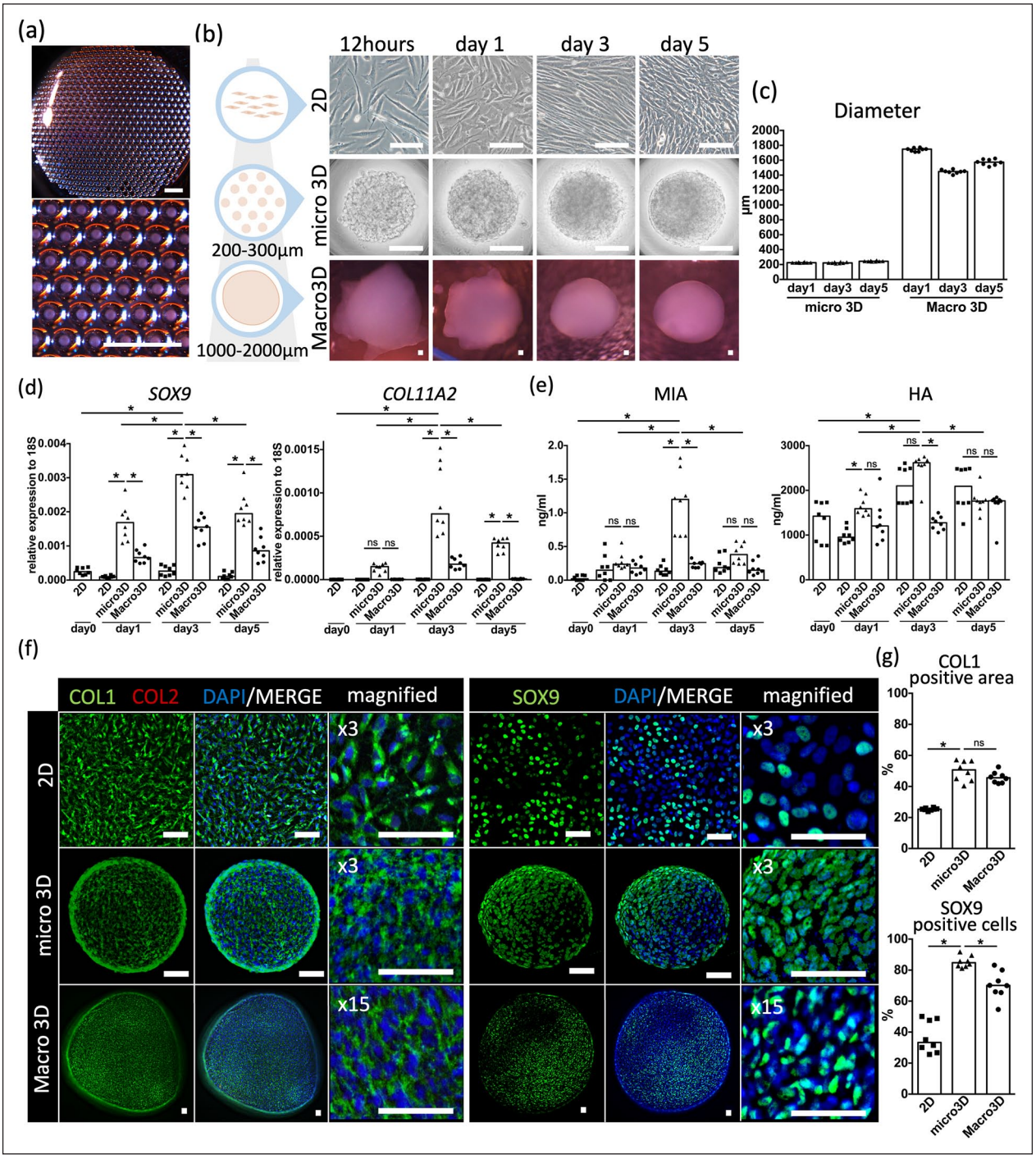

Figure 2. Comparison of 2D, micro 3D, and macro 3D cultures. (a) Image of micro 3D culture with a magnified panel below. Scale bars: 2 mm. (b) Time course images of 2D (top row), micro 3D (middle row), and macro 3D (bottom row) cultures. Scale bars: 100 μm. (c) Diameter of micro 3D and macro 3D spheroids. (d) Gene expression of SOX9 and COLL11A2 against 18S in each culture system on a time course. (e) Secretion level of melanoma inhibitory activity (MIA) and hyaluronic acid (HA) in each culture system on a time course. (f) Merged and magnified immunohistochemical images of 2D (top row), micro 3D (middle row), and macro 3D (bottom row) cultures after staining with type I collagen (COL1) (green), type II collagen (COL2) (red) (left panels), and SOX9 (green) (right panels), along with diamidino-phenylindole (DAPI) (blue). Scale bars: 50 μm. (g) Areas positive for COL1 staining (%) and cells positive for SOX9 staining (%) based on immunohistochemical images of each culture system. Data are shown from eight independent experiments.

ns: not significant.

*$p < 0.01$.

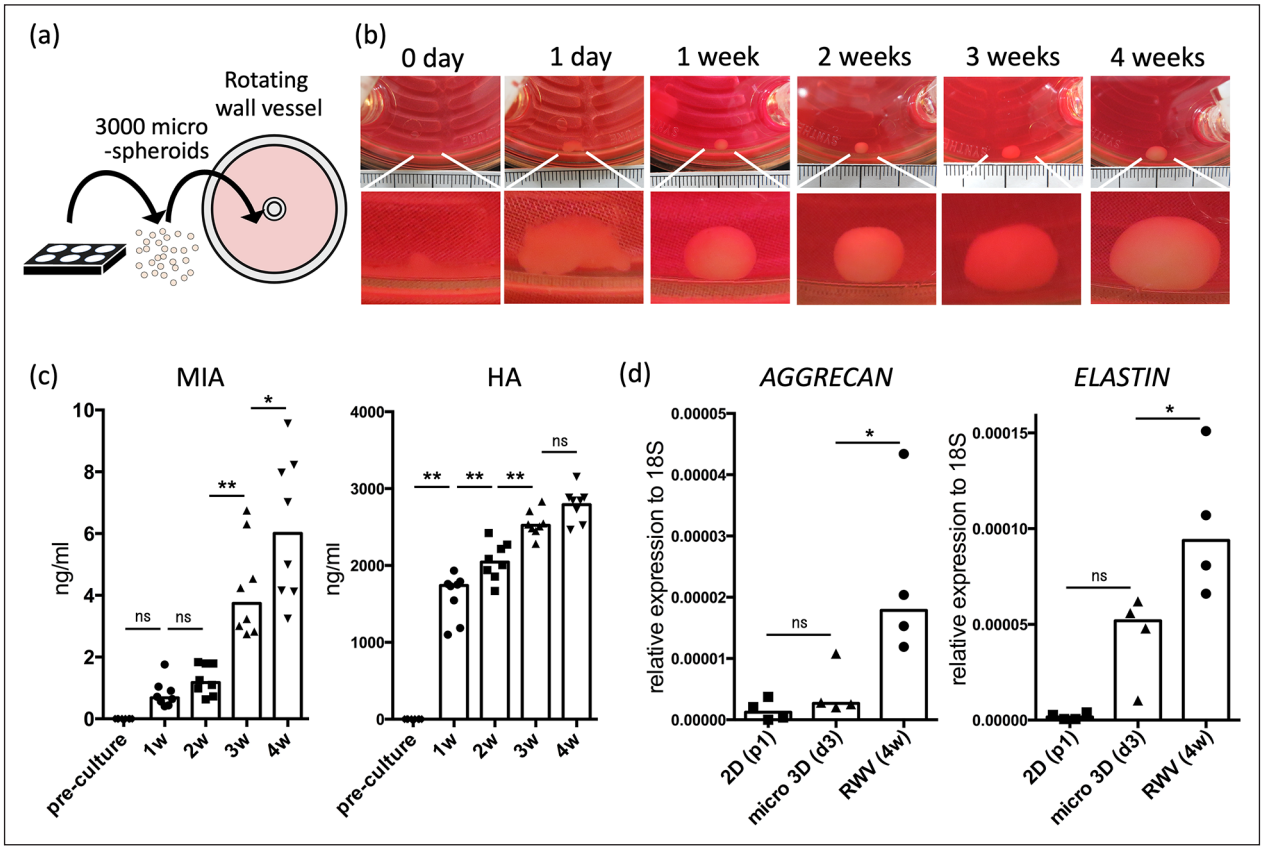

Figure 3. Maturation of fused micro 3D–cultured spheroids into elastic cartilage via rotating wall vessel (RWV) culture. (a) Schematic representation of micro 3D–cultured spheroids transferred into an RWV. (b) Representative image of tissue cultured in an RWV. Scale bars: 1 mm (c) Secretion level of melanoma inhibitory activity (MIA) and hyaluronic acid (HA) on a time course ($n = 8$). (d) Gene expression of AGGRECAN and ELASTIN against 18S in passage 2 chondroprogenitor cells, day 3 micro 3D–cultured spheroids and week 4 RWV–cultured cartilage ($n = 4$).
ns: not significant.
*$p < 0.05$. **$p < 0.01$.

significant differences were observed in comparison with 2D culture (Figure 2(e)). In micro 3D culture, the expression of *SOX9* and *COL11A2* and the level of MIA and HA secretion were significantly higher on day 3 than on days 1 and 5 (Figure 2(d) and (e)). These results suggest that micro 3D culture enhances chondrogenesis and that the performance of the system peaks at 3 days of culture.

The auricular hillocks exhibited a mesenchymal, prechondral character. Therefore, we analyzed each culture method by performing immunohistochemistry analysis of type I collagen, type II collagen, and SOX9 (Figure 2(f)). Positive type I collagen staining was observed in all culture systems (2D culture, 25.4% (24.9%–26.0%); micro 3D culture, 50.7% (44.1%–56.4%); macro 3D culture, 45.6% (42.5%–48.1%)). Type II collagen was not detected in any of the culture systems. These findings were consistent with the immunohistochemistry results for the E11.5 embryonic auricular hillocks (Figures 1(c) and 2(f)). The micro 3D–cultured spheroids were 84.8% (82.5%–88.7%) positive for SOX9, a significantly higher proportion than that observed in the 2D culture (33.3% (27.6%–48.5%)) and macro 3D culture (70.1% (65.6%–78.3%)) (Figure 2(g)). These results indicate that micro 3D–cultured spheroids have a mesenchymal character and a higher chondrogenic potential than 2D cultured–spheroids and macro 3D–cultured spheroids.

Rotating wall vessel culture and in vitro analysis

To promote further chondrogenesis and produce an elastic cartilage tissue, we transferred 3000 spheroids of day 3 micro 3D culture into a rotating wall vessel and allowed 12 h for fusion, followed by 4 weeks of rotation culture, which has been reported to be effective for inducing chondrogenesis (Figure 3(a), Supplemental Video 2).[16] The spheroids fused into a tissue within a week, after which the tissue exhibited a weekly increase in size (Figure 3(b)). ELISA of the culture medium revealed significantly increasing levels of MIA, which is secreted by developing cartilage,[29,30] at weeks 3 and 4 of rotating

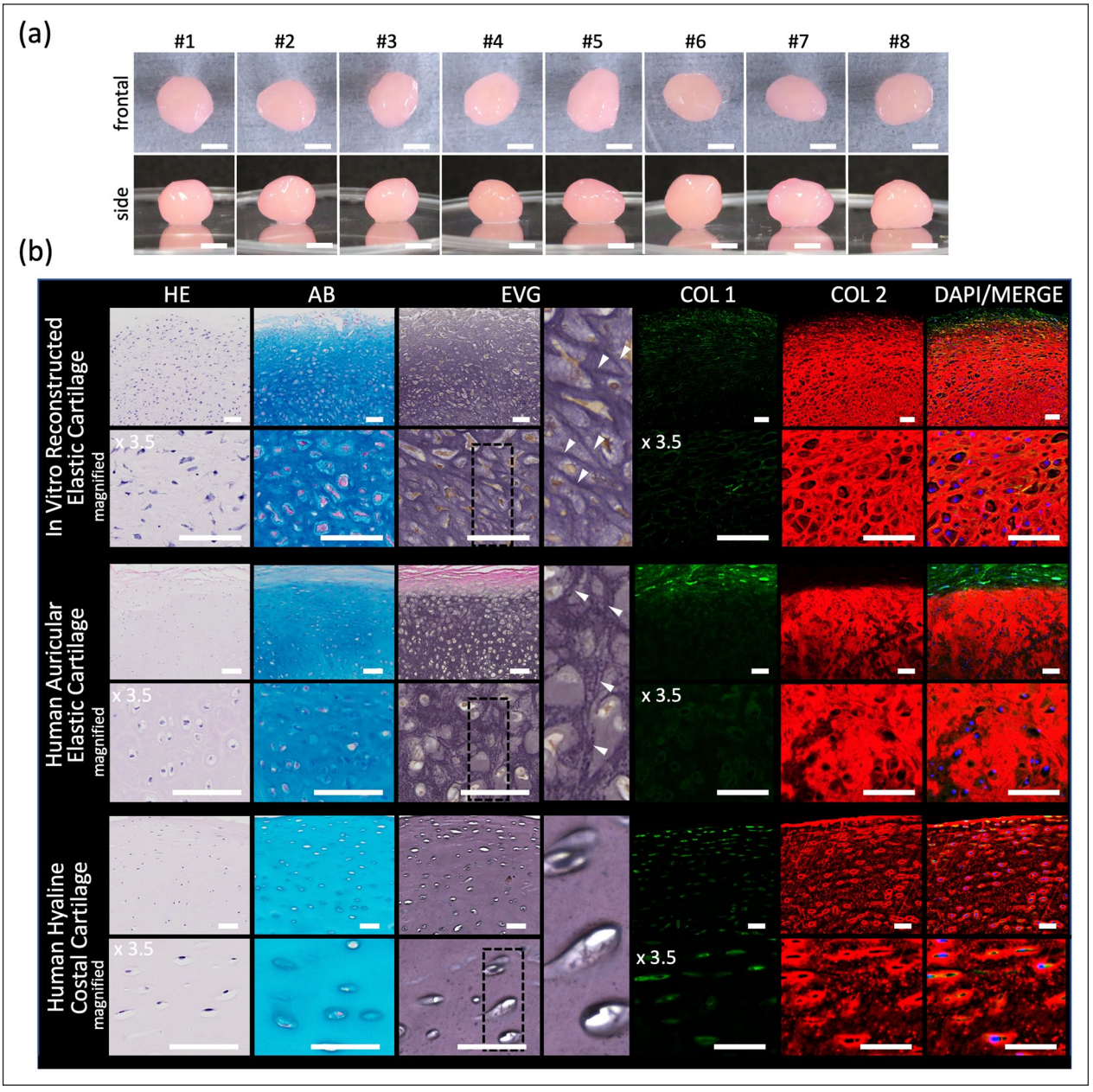

Figure 4. Characterization of in vitro human perichondrial chondroprogenitor cell–derived reconstructed elastic cartilage. (a) Images of the frontal and side view. Scale bars: 2 mm. (b) Histological images of in vitro reconstructed elastic (top row), human auricular (middle row), and human costal (bottom row) cartilages stained with HE, Alcian blue (AB), Elastica Van Gieson (EVG), type I collagen (COL1) (green), type II collagen (COL2) (red), and diamidino-phenylindole (DAPI) (blue), each with magnified images below. Elastica Van Gieson (EVG) panels have further magnified panels of the section with dashed lines with white arrowheads indicating elastic fibers. Scale bars: 50 μm.

wall vessel culture. Levels of HA, which is abundant in elastic cartilage,[31] progressively increased until week 3; no significant differences were observed at week 4 (Figure 3(c)). The expression of *AGGRECAN* and *ELASTIN* were significantly higher in week 4 cartilage than in day 3 micro 3D spheroids (Figure 3(d)). These results indicate the benefit of using rotating wall vessel culture to promote cartilage maturation, consistent with previous reports.[16,32,33]

After 4 weeks of rotating wall vessel culture, the reconstructed elastic cartilage reached 4.3 mm (3.9–4.5 mm) in diameter (Figures 4(a) and 5(e)). Histological analysis revealed positive Alcian blue, EVG, and type II collagen staining, which was consistent with the results for the human native auricular cartilage. The reconstructed elastic cartilage also showed inconsistent EVG staining pattern with the human native costal hyaline cartilage (Figure 4(b)). Elastic modulus measurements of

the reconstructed elastic cartilage were also consistent with those of human native auricular elastic cartilage (Figure 5(f)). These results indicate that our novel method of using micro 3D culture followed by rotating wall vessel culture can be used to successfully reconstruct a scaffold-free elastic cartilage tissue from human auricular perichondrial cells in vitro.

Craniofacial implantation treatments and in vivo analysis

To evaluate whether the reconstructed elastic cartilage exhibited morphological stability after craniofacial transplantation, the cartilage was transplanted into the subcutaneous layer of the forehead in immunosuppressed mice (Figure 5(a)). The transplantation group exhibited significantly increased superficial thickness in the forehead immediately following surgery and 2 months after, compared with the sham surgery group (Figure 5(b)). The elastic cartilage was extracted 2 months after transplantation (Figure 5(c)). The ex vivo elastic cartilage was 4.2 mm (3.8–4.4 mm) in diameter. When compared with the in vitro elastic cartilage, there was no significant difference in size (Figure 5(e)). Furthermore, no significant differences were observed between the elastic moduli of the in vitro and ex vivo elastic cartilage (Figure 5(f)). The ex vivo elastic cartilage was positive for Alcian blue, EVG, and type II collagen staining, similar to the in vitro cartilage (Figure 5(g)). Overall, these results indicated that the reconstructed elastic cartilage exhibited morphological stability without shrinkage when used for craniofacial transplantation.

Discussion

The development of morphologically stable, scaffold-free reconstructed elastic cartilage tissue is necessary to improve treatments for craniofacial defects. However, mesenchymal condensation, which occurs during chondrogenesis, poses a challenge with in vivo maturating methods. Therefore, we propose a method in which chondrogenesis is completed in vitro, to avoid shrinkage after transplantation. To our knowledge, this study is the first to demonstrate the in vitro production of human auricular perichondrial chondroprogenitor cell–derived elastic cartilage via micro 3D culture (Figure 6).

Despite the advantages of auricular perichondrial chondroprogenitor cells, few reconstruction methods have been reported, whereas numerous methods using auricular cells have been described. This could be attributed to the difficulty of detaching the auricular perichondrium from the auricle and isolating the chondroprogenitor cells. However, we succeeded in isolating a high percentage of perichondrial chondroprogenitor cells (Figure 1(f)), and our results may encourage further attempts. The success of our novel reconstruction method can be partially ascribed to the use of auricular perichondrial chondroprogenitor cells. Experiments comparing the potential of auricular chondrocytes and auricular perichondrium–derived chondroprogenitor cells may be beneficial for optimizing this method.

Mimicking the embryonic process is a principal approach to tissue reconstruction. Most elastic cartilage protocols mimic the embryonic process in a chemical manner by using differentiation factors to mimic cell-to-cell cytokine reactions. Cytokines such as TGFβ, PDGF-BB, FGF-2, and IGF have been reported to improve chondrogenesis, and we used several cytokines in this study.[10,33–38] In contrast, mimicking morphological factors such as embryonic size and shape has not been frequently attempted; handling 3D structures on a microscopic scale is more difficult than simply adding cytokines to the medium. In this study, the mouse auricle originated from emerging auricular hillocks, which were 200–300 μm in size with mesenchymal characteristics, moderately similar to previously reported human auricular hillocks (Figure 1(a)–(c)).[22] The morphological characteristics of the auricular hillocks may play an important role in early auricular chondrogenesis, despite the differences between human and mouse auricles in terms of the final size and shape. Thus, mimicking the morphological characteristics of the auricular hillocks may have contributed to the increased expression of chondrogenic induction factors observed in the micro 3D culture system. Our results demonstrated that mimicking the embryonic process in a morphological manner is an important aspect of elastic cartilage engineering; this finding may be applicable to the engineering of other tissue types, as well.

SOX9 is a key factor in both chondrogenesis and mesenchymal condensation in cartilage development throughout the body. In particular, SOX9 plays a major role in regulating chondrogenesis in the craniofacial area, including in neural crest–derived phalangeal arches, from which auricular hillocks originate.[23–25] Heterozygous mutations in the human *SOX9* gene cause campomelic dysplasia, which results in low-set dysplastic ears.[39,40] Therefore, we evaluated SOX9 expression in mouse embryos and micro 3D culture. One of the limitations of our study was that the cell density of the auricular hillocks, which may be an important morphological factor, was not examined. However, the feasibility of evaluating cell density in the auricular hillocks and controlling cell density using centrifugation at the micro scale is uncertain. The self-aggregation method used in this study was selected over methods involving centrifugation because cell-to-cell aggregation obviously occurs without centrifugal force during natural embryogenesis.

As mentioned, owing to the difficulty of handling microscopic 3D structures, the morphological features of cultured spheroids may vary widely, and creating a reliable method for both clinical and laboratory use is

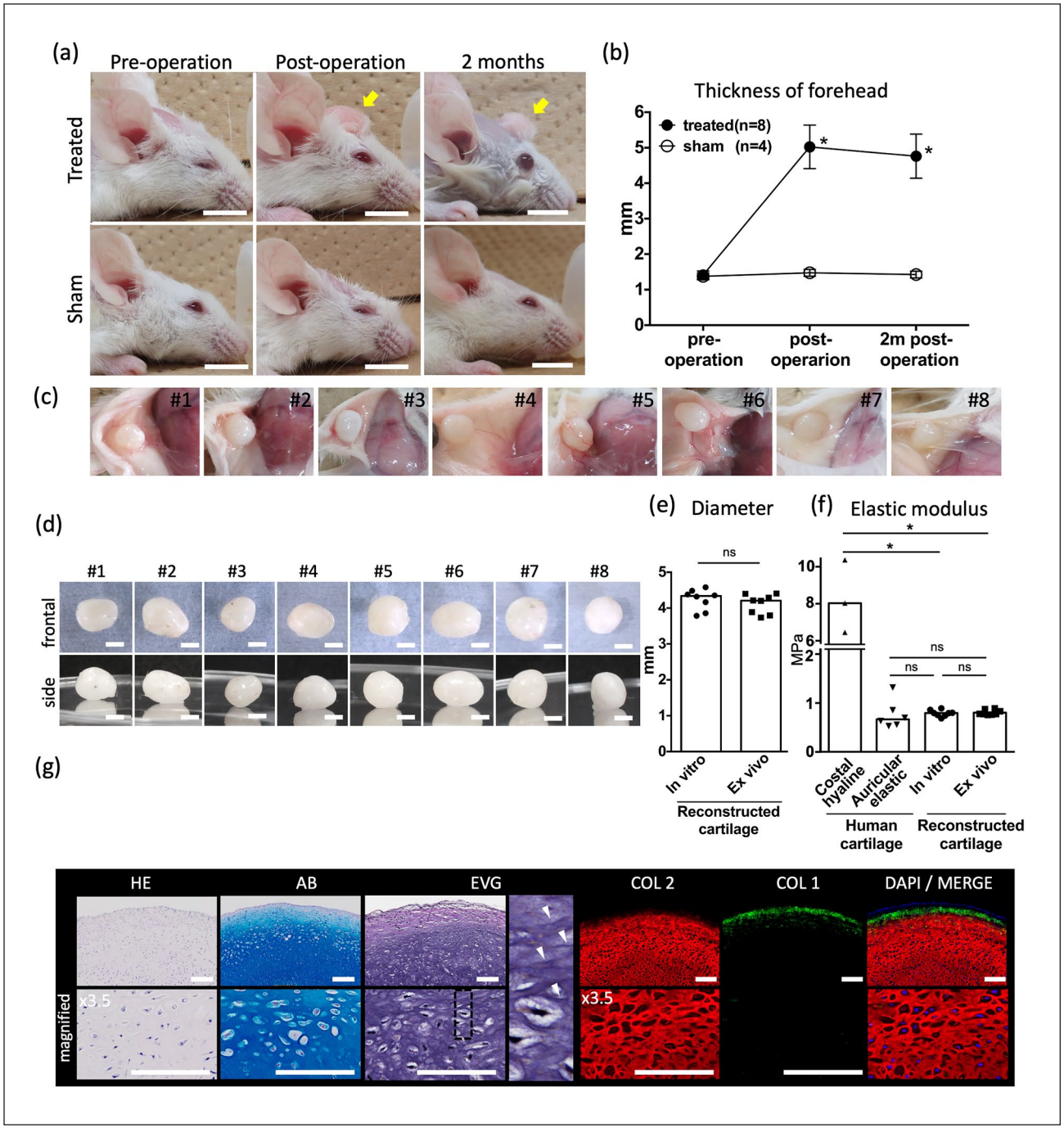

Figure 5. Craniofacial implantation treatments and in vivo analysis. (a) Representative images of the craniofacial area of elastic cartilage–implanted mice (upper row) and sham-treated mice (lower row), with (b) measured forehead thickness. Scale bars: 1 cm. Yellow arrows: Implanted elastic cartilage. Data are shown as the mean ± SD. (c) In vivo images of the implanted elastic cartilage after 2 months of transplantation. (d) Images of the frontal view and side view of the ex vivo elastic cartilage. Scale bars: 2 mm. (e) Diameter of in vitro and ex vivo elastic cartilage. (f) Elastic modulus of human costal hyaline cartilage, human auricular elastic cartilage, in vitro, elastic cartilage reconstruction and ex vivo elastic cartilage reconstruction. (g) Histological images of ex vivo elastic cartilage reconstruction stained with HE, Alcian blue (AB), Elastica Van Gieson (EVG), type I collagen (COL1) (green), type II collagen (COL2) (red), and diamidino-phenylindole (DAPI) (blue), each with magnified images below. Elastica Van Gieson (EVG) panels have further magnified panels of the section with dashed lines with white arrowheads indicating elastic fibers. Scale bars: 50 μm. $n = 8$ mice for the treated group, and $n = 4$ mice for the sham-treated group.

ns: not significant.

*$p < 0.01$.

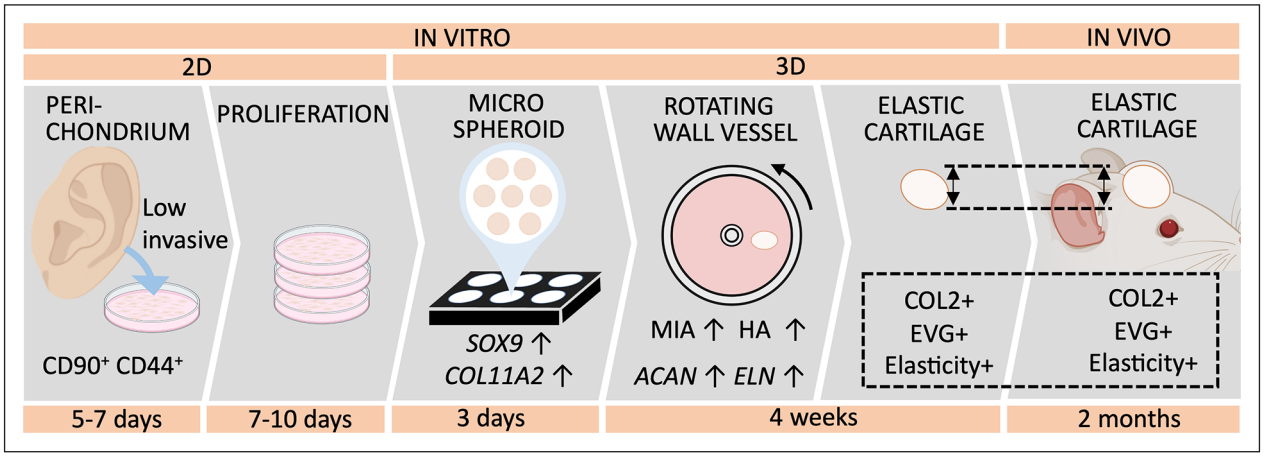

Figure 6. Protocol for reconstructing elastic cartilage tissue using human auricular perichondrial chondroprogenitor cells.

difficult because of unstable results. However, the micro 3D–cultured spheroids created in our study exhibited low variability on day 3, without requiring a high level of technical skill (Figure 2(c)). Day 3 micro 3D–cultured spheroids exhibited better results than day 5 micro 3D–cultured spheroids (Figure 2(d) and (e)). Attachment to the culture plate on day 5 may be one of the reasons for this observation (Supplemental Figure 1(b)). Preventing this phenomenon may produce different results.

Exposing tissues to shear stress by using bioreactors has also been reported to be an effective culture method for elastic cartilage reconstruction.[16,32,33] Our results also indicated that this is a promising method, based on the progressive increase in chondrogenesis-related protein secretion levels and the in vitro histological analysis of elastic cartilage cultured via rotating wall vessel. Surprisingly, 3000 micro 3D–cultured spheroids fused together within a day strongly enough to tolerate a speed of 15 rpm (Figure 3(b)). Success in generating spheroids that exhibited high SOX9 expression may explain this result. Further studies should assess the effects of using different numbers of spheroids for the fusion step.

The morphological stability of engineered tissues in terms of size, shape, and stiffness is crucial when performing craniofacial transplantations, because the results are particularly noticeable. In our previous study, we created a scaffold-free human perichondrium–derived pre-cartilage structure in vitro that exhibited shrinkage after maturing into elastic cartilage in vivo.[16] Condensation during cartilage differentiation, which occurred after transplantation, may have caused the shrinkage. In this study, the cartilage exhibited significant morphological stability when transplanted in craniofacial sites; the size of the sample was maintained post operation (Figure 5(e)). The completion of differentiation in vitro may explain this major improvement. The mechanical measurement results supported these findings. The human auricular elastic cartilage had a lower elastic modulus than human costal hyaline cartilage, which was consistent with previous studies.[5] The elastic modulus of our reconstructed elastic cartilage was similar to that of human native elastic cartilage and was maintained after transplantation (Figure 5(f)). However, the transplanted elastic cartilage was not subjected to long-term observation in this study; this should be considered in the future. Additionally, the reconstructed elastic cartilage was simple in shape, and future goals include establishing a method for creating more complex elastic cartilage structures.

Conclusions

In summary, we established an efficient culture method for promoting chondrogenic induction by using micro 3D–cultured spheroids to morphologically mimic auricular hillocks. Using this method, we succeeded in developing human auricular perichondrial chondroprogenitor cell–derived elastic cartilage in vitro that exhibits superficial effects when transplanted craniofacially, without major post-transplantation shrinkage. Micro 3D–cultured spheroids may be a useful tool for further exploring auricular development, which remains poorly understood. Furthermore, this novel elastic cartilage reconstruction method may contribute to the future treatment of patients with external auricular disorders.

Acknowledgements

We thank Y. Terado, M. Tanaka, C. Ikezuki, M. Yajima, K. Saito, J. Shibasaki, T. Kobayashi, Y. Kawakatsu, H. Nozawa, N. Mizuguchi, and Y. Nafune for providing technical support and the members of our laboratory for their comments. We would like to thank Editage (https://www.editage.com/) for editing and reviewing this manuscript for English language.

Author contributions

TO designed the study, carried out cell culture, analyzed the data, and drafted the manuscript. SK (Kobayashi), KY, and SK (Kagimoto) obtained, isolated, and analyzed chondroprognitor

cells. SO and YU performed embryonic analysis and histological analysis. MM, and TT carried out animal transplantation, and histological analysis. YI and HT supervised the project and critically reviewed the manuscript.

Declaration of conflicting interests

The author(s) declared no potential conflicts of interest with respect to the research, authorship, and/or publication of this article.

Funding

The author(s) disclosed receipt of the following financial support for the research, authorship, and/or publication of this article: This work was supported by the Japan Agency for Medical Research and Development (AMED) under grant number JP21lm0203122h0002. This work was also supported by Terumo Life Science Foundation under grant number 19-T001.

ORCID iDs

Takayoshi Oba https://orcid.org/0000-0002-1865-5940
Shinji Kobayashi https://orcid.org/0000-0003-2058-5678

Supplemental material

Supplemental material for this article is available online.

Data availability

The data and procedure in this study are included in article and supplementary material. Further requirements can be available from the corresponding author on request.

References

1. Luquetti DV, Leoncini E and Mastroiacovo P. Microtia-anotia: a global review of prevalence rates. *Birth Defects Res A Clin Mol Teratol* 2011; 91: 813–822.
2. Luquetti DV, Heike CL, Hing AV, et al. Microtia: epidemiology and genetics. *Am J Med Genet A* 2012; 158: 124–139.
3. Mastroiacovo P, Corchia C, Botto LD, et al. Epidemiology and genetics of microtia-anotia: a registry based study on over one million births. *J Med Genet* 1995; 32: 453–457.
4. Bly RA, Bhrany AD, Murakami CS, et al. Microtia reconstruction. *Facial Plast Surg Clin North Am* 2016; 24: 577–591.
5. Griffin MF, O'Toole G, Sabbagh W, et al. Comparison of the compressive mechanical properties of auricular and costal cartilage from patients with microtia. *J Biomech* 2020; 103: 109688.
6. Zhang L, He A, Yin Z, et al. Regeneration of human-ear-shaped cartilage by co-culturing human microtia chondrocytes with BMSCs. *Biomaterials* 2014; 35: 4878–4887.
7. Fulco I, Miot S, Haug MD, et al. Engineered autologous cartilage tissue for nasal reconstruction after tumor resection. An observational first-in-human trial. *Clin Trial* 2014; 384: 337–346.
8. Reiffel AJ, Kafka C, Hernandez KA, et al. High-fidelity tissue engineering of patient-specific auricles for reconstruction of pediatric microtia and other auricular deformities. *PLoS One* 2013; 8: e56506.
9. Jessop ZM, Javed M, Otto IA, et al. Combining regenerative medicine strategies to provide durable reconstructive options: auricular cartilage tissue engineering. *Stem Cell Res Ther* 2016; 7: 19.
10. Shieh SJ, Terada S and Vacanti JP. Tissue engineering auricular reconstruction: in vitro and in vivo studies. *Biomaterials* 2004; 25: 1545–1557.
11. Liu Y, Zhang L, Zhou G, et al. In vitro engineering of human ear-shaped cartilage assisted with CAD/CAM technology. *Biomaterials* 2010; 31: 2176–2183.
12. Bichara DA, O'Sullivan NA, Pomerantseva I, et al. The tissue-engineered auricle: past, present, and future. *Tissue Eng Part B Rev* 2012; 18: 51–61.
13. Isogai N, Asamura S, Higashi T, et al. Tissue engineering of an auricular cartilage model utilizing cultured chondrocyte-poly(L-lactide-epsilon-caprolactone) scaffolds. *Tissue Eng* 2004; 10: 673–687.
14. Giardini-Rosa R, Joazerio PP, Thomas K, et al. Development of scaffold-free elastic cartilaginous constructs with structural similarities to auricular cartilage. *Tissue Eng Part A* 2014; 20: 1012–1026.
15. Akbari P, Waldman SD, Cushing SL, et al. Bioengineering pediatric scaffold-free auricular cartilaginous constructs. *Laryngoscope* 2017; 127: 153–158
16. Enomura M, Murata S, Terado Y, et al. Development of a method for scaffold-free elastic cartilage creation. *Int J Mol Sci* 2020; 21: 8496.
17. Hall BK and Miyake T. Divide, accumulate, differentiate: cell condensation in skeletal development revisited. *Int J Dev Biol* 1995; 39: 881–893.
18. Hall BK and Miyake T. All for one and one for all: condensations and the initiation of skeletal development. *Bioessays* 2000; 22: 138–147.
19. Kobayashi S, Takebe T, Zheng YW, et al. Presence of cartilage stem/progenitor cells in adult mice auricular perichondrium. *PLoS One* 2011; 6: e26393.
20. Kobayashi S, Takebe T, Inui M, et al. Reconstruction of human elastic cartilage by a CD44+ CD90+ stem cell in the ear perichondrium. *Proc Natl Acad Sci USA* 2011; 108: 14479–14484.
21. Wood-Jones F and I-Chuan W. The development of the external ear. *J Anat* 1934; 68: 525–533.
22. Veugen CCAFM, Dikkers FG and de Bakker BS. The developmental origin of the auricula revisited. *Laryngoscope* 2020; 130: 2467–2474.
23. Cox TC, Camci ED, Vora S, et al. The genetics of auricular development and malformation: new findings in model systems driving future directions for microtia research. *Eur J Med Genet* 2014; 57: 394–401.
24. Rau MJ, Fischer S and Neumann CJ. Zebrafish Trap230/Med12 is required as a coactivator for Sox9-dependent neural crest, cartilage and ear development. *Dev Biol* 2006; 296: 83–93.
25. Mori-Akiyama Y, Akiyama H, Rowitch DH, et al. Sox9 is required for determination of the chondrogenic cell lineage in the cranial neural crest. *Proc Natl Acad Sci USA* 2003; 100: 9360–9365.
26. Bridgewater LC, Lefebvre V and de Crombrugghe B. Chondrocyte-specific enhancer elements in the Col11a2 gene resemble the Col2a1 tissue-specific enhancer. *J Biol Chem* 1998; 273: 14998–15006.

27. Baas D, Malbouyres M, Haftek-Terreau Z, et al. Craniofacial cartilage morphogenesis requires zebrafish col11a1 activity. *Matrix Biol* 2009; 28: 490–502.
28. Temtamy SA, Männikkö M, Abdel-Salam GM, et al. Otospondylo-megaepiphyseal dysplasia (OSMED): clinical and radiological findings in sibs homozygous for premature stop codon mutation in the COL11A2 gene. *Am J Med Genet A* 2006; 140: 1189–1195.
29. Bosserhoff AK, Kondo S, Moser M, et al. Mouse CD-RAP/MIA gene: structure, chromosomal localization, and expression in cartilage and chondrosarcoma. *Dev Dyn* 1997; 208: 516–525.
30. Lougheed JC, Holton JM, Alber T, et al. Structure of melanoma inhibitory activity protein, a member of a recently identified family of secreted proteins. *Proc Natl Acad Sci USA* 2001; 98: 5515–5520.
31. Wusteman FS and Gillard GC. Hyaluronic acid in elastic cartilage. *Experientia* 1977; 33: 721–723.
32. Takebe T, Kobayashi S, Kan H, et al. Elastic cartilage engineering from cartilage progenitor cells using rotating wall vessel bioreactor. *Transplant Proc* 2012; 44: 1158–1161.
33. Ohyabu Y, Tanaka J, Ikada Y, et al. Cartilage tissue regeneration from bone marrow cells by RWV bioreactor using collagen sponge scaffold. *Mater Sci Eng C* 2009; 29: 1150–1155.
34. Nayyer L, Patel KH, Esmaeili A, et al. Tissue engineering: revolution and challenge in auricular cartilage reconstruction. *Plast Reconstr Surg* 2012; 129: 1123–1137.
35. Mendes LF, Katagiri H, Tam WL, et al. Advancing osteochondral tissue engineering: bone morphogenetic protein, transforming growth factor, and fibroblast growth factor signaling drive ordered differentiation of periosteal cells resulting in s cartilage and bone formation in vivo. *Stem Cell Res Ther* 2018; 9: 42.
36. Wang Y, Kim UJ, Blasioli DJ, et al. In vitro cartilage tissue engineering with 3D porous aqueous-derived silk scaffolds and mesenchymal stem cells. *Biomaterials* 2005; 26: 7082–7094.
37. Tay AG, Farhadi J, Suetterlin R, et al. Cell yield, proliferation, and postexpansion differentiation capacity of human ear, nasal, and rib chondrocytes. *Tissue Eng* 2004; 10: 762–770.
38. Hicks DL, Sage AB, Shelton E, et al. Effect of bone morphogenetic proteins 2 and 7 on septal chondrocytes in alginate. *Otolaryngol Head Neck Surg* 2007; 136: 373–379.
39. Meyer J, Südbeck P, Held M, et al. Mutational analysis of the SOX9 gene in campomelic dysplasia and autosomal sex reversal: lack of genotype/phenotype correlations. *Hum Mol Genet* 1997; 6: 91–98.
40. Lee YH and Saint-Jeannet JP. Sox9 function in craniofacial development and disease. *Genesis* 2011; 49: 200–208.